MICROCOPY RESOLUTION TEST CHART
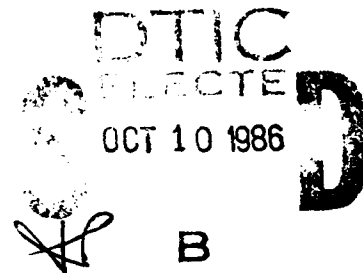NATIONAL BUREAU OF STANDARDS-1963-A

Proton Beam Deposition, Heating, and Radiation from an Iron Plasma

J. E. ROGERSON AND R. W. CLARK

Plasma Radiation Branch
Plasma Physics Division

DTIC
ELECTE
OCT 10 1986

B

86 10 9 024

AD-A172 947

REPORT DOCUMENTATION PAGE

1a. REPORT SECURITY CLASSIFICATION UNCLASSIFIED	1b RESTRICTIVE MARKINGS		
2a. SECURITY CLASSIFICATION AUTHORITY	3. DISTRIBUTION/AVAILABILITY OF REPORT Approved for public release; distribution unlimited.		
2b DECLASSIFICATION/DOWNGRADING SCHEDULE			
4. PERFORMING ORGANIZATION REPORT NUMBER(S) NRL Memorandum Report 5846	5. MONITORING ORGANIZATION REPORT NUMBER(S)		

6a NAME OF PERFORMING ORGANIZATION Naval Research Laboratory	6b. OFFICE SYMBOL (If applicable) Code 4720	7a. NAME OF MONITORING ORGANIZATION
6c. ADDRESS (City, State, and ZIP Code) Washington, DC 20375-5000		7b. ADDRESS (City, State, and ZIP Code)

8a. NAME OF FUNDING/SPONSORING ORGANIZATION Defense Nuclear Agency	8b. OFFICE SYMBOL - (If applicable) RAEV	9. PROCUREMENT INSTRUMENT IDENTIFICATION NUMBER

8c. ADDRESS (City, State, and ZIP Code) Alexandria, VA 22310	10. SOURCE OF FUNDING NUMBERS			
	PROGRAM ELEMENT NO. 62715H	PROJECT NO.	TASK NO. RL RA	WORK UNIT ACCESSION NO. DN880-191

11. TITLE (Include Security Classification)

Proton Beam Deposition, Heating, and Radiation from an Iron Plasma

12. PERSONAL AUTHOR(S)
Rogerson, J.E. and Clark, R.W.

13a. TYPE OF REPORT Interim	13b. TIME COVERED FROM _____ TO _____	14. DATE OF REPORT (Year, Month, Day) 1986 September 19	15. PAGE COUNT 26

16. SUPPLEMENTARY NOTATION
(See Page ii)

17.	COSATI CODES		18. SUBJECT TERMS (Continue on reverse if necessary and identify by block number)
FIELD	GROUP	SUB-GROUP	Ion beam Stopping power
			Plasma Radiation transport

19. ABSTRACT (Continue on reverse if necessary and identify by block number)

A fully self consistent one dimensional ion beam-slab interaction model has been applied to the investigation of the interaction of an energetic proton beam with an iron slab target. This model describes the slowing down of the beam, the hydrodynamic response and ionization dynamics of the slab, and detailed radiation emission and transport. An extensive atomic level structure with collisional radiative ionization dynamics is employed. A hybrid radiation transport algorithm consisting of a multifrequency formalism for the continuum and a probabilistic treatment of lines is used. The evolution of the Fe plasma with time is described. Calculated spectral emissions from the front and rear surfaces are presented at various times in the interaction.

20 DISTRIBUTION/AVAILABILITY OF ABSTRACT ☒ UNCLASSIFIED/UNLIMITED ☐ SAME AS RPT. ☐ DTIC USERS	21. ABSTRACT SECURITY CLASSIFICATION UNCLASSIFIED	
22a NAME OF RESPONSIBLE INDIVIDUAL Dr. Jack Davis	22b TELEPHONE (Include Area Code) (202) 767-3278	22c. OFFICE SYMBOL Code 4720

DD FORM 1473, 84 MAR   83 APR edition may be used until exhausted.
All other editions are obsolete

☆U.S. Government Printing Office: 1986—607-047

16. SUPPLEMENTARY NOTATION
This work was supported by the Defense Nuclear Agency under Task Code and Title
RL RA/Advanced Simulation Concepts, work unit 00049 and work unit Title "X-Ray Source
Development Theory." MIPR NO. 86-570.

CONTENTS

PROTON BEAM DEPOSITION, HEATING, AND RADIATION FROM AN IRON PLASMA

I. Introduction

With current charged particle beam technologies, it is possible to bombard targets with intense proton beams. The interest in charged particle beam-target interactions is enhanced by the expectation that the beam-target energy coupling can be understood and modelled, to first approximation, in terms of well understood classical, linear processes, as opposed to the non-linear effects involved in laser-target coupling.[1] Thus, much effort is directed toward investigating these phenomena. Significant applications of this research include the use of ion beams for x-ray generation, inertial confinement fusion, and weapons lethality and vulnerability studies.

II. Theoretical Model

The interaction of a monoenergetic one MeV proton beam with a planar aluminum slab of 15 μm thickness has been previously investigated.[2] This beam was assumed to consist of a square-shaped pulse of 10 nanosecond duration with a flux of 10^{26} protons cm^{-2} sec^{-1}. The beam intensity on target was 1.6×10^{13} W/cm^2, which is comparable to intensities available with current pulsed-power generators.

In the present study, the interaction of this same proton beam with a planar 8.0-μm-thick iron slab is treated. This distance approximately corresponds to the range of a one MeV proton in cold solid density Fe^3.

The scheme for treating the proton beam-iron slab interaction is fundamentally the same as that described in Ref. 2 for treating the proton beam-Al slab interaction. The hydrodynamic response is treated via a one-dimensional model with a sliding-zone version of flux corrected transport. A special gridding algorithm moves zones in a Lagrangian fashion and adjusts the mesh in order to resolve steep gradients in the flow. A single temperature model is employed, since equilibration times are generally short compared with hydrodynamic timescales in this problem. A collisional radiative equilibrium treatment is used to obtain the atomic

level populations. Radiation transport is treated with a hybrid scheme which uses multifrequency ray tracing for the continua, and a probability-of-escape method for lines. The radiation transport is coupled self-consistently into the ionization dynamics. The proton stopping power includes contributions from bound atomic electrons, free plasma electrons, and plasma ions. These features are discussed in detail in Ref. 2.

The Fe atomic model used in this calculation did not have excited level structure in ionization stages below Fe XVI. Only ground states were carried for stages I through XV. While this lack of level structure and the resulting omission of lines from the radiation transport scheme can modify the energy balance in regimes where these lower stages are highly populated, it is estimated that the effect is less than a factor of two on the energy lost due to radiation.

A major difference between this work with Fe as the target material and the previous work with Al as the target material is in the treatment of the bound electron stopping power. For the proton-Al^{+q} interaction, where q is the ionic charge, detailed stopping power cross sections are available;[4] for the proton-Fe^{+q} interaction, no such data are currently available. In the present treatment, stopping power due to bound electrons is calculated from a method proposed by Mehlhorn.[5] In this approach, stopping power is calculated from the Bethe equation (which is valid at high projectile energies) and from the LSS model (which is valid in the low projectile energy regime); then the stopping cross section is taken to be the lesser of these two results; i.e.,

$$S_b(E) = \min \left[S_{Bethe}(E), S_{LSS}(E) \right] .$$

Mehlhorn[5] has found that, by including shell corrections in the Bethe equation, he can adequately represent cold target stopping power results. By applying this model to cold solid density Fe, it has been verified that the Andersen-Ziegler[3] results for proton stopping power can be reproduced very well.

The Bethe model for the stopping cross section is given by[5]

$$S_{Bethe}(E) = \frac{4\pi Z_B^2 (Z-\bar{Z})e^4}{mV^2} \left\{ \ln\Lambda - \beta^2 - \sum_{i=0}^{4} b_i [\log(E)]^i \right\} ,$$

where $\Lambda = \frac{2\pi mV^2}{\langle I \rangle} \gamma^2 .$

2

Here Z_B is the effective charge of the projectile ion, Z is the atomic number of the target, $\bar{Z}$ is the average charge of the target ions, e and m are the electron charge and rest mass, E and V are the projectile energy and velocity, $\beta = V/c$, where c is the vacuum velocity of light, <I> is the average ionization potential of the target ions, and the b_i are least-squares fit parameters derived by Andersen and Ziegler[3] to calculate shell corrections to the Bethe stopping power.

$$\gamma = (1-\beta^2)^{-1/2} .$$

The LSS model is described by the following equations:[5]

$$S_{LSS}(E) = \left\{ \frac{0.0793 \, Z_B^{2/3} \, (Z-\bar{Z})^{1/2} \, (1+A)^{3/2}}{(Z_B^{2/3} + (Z-\bar{Z})^{2/3})^{3/4} \, A_2^{1/2}} \right\} \frac{\sqrt{E_L}}{R_L} \sqrt{E}$$

$$\text{where} \quad E_L = \frac{Z_B(Z-\bar{Z}) \, (1+A)e^2}{0.4683 \times 10^{-8} A} \times \left[Z_B^{2/3} + (Z-\bar{Z})^{2/3} \right]^{1/2} ,$$

$$R_L = \frac{(1+A)^2}{4\pi A} \frac{\left[Z_B^{2/3} + (Z-\bar{Z})^{2/3} \right]}{0.219 \times 10^{-16}} .$$

$A = A_2/A_1$, where A_2 is the atomic weight of the target ion, and A_1 is the atomic weight of the projectile ion.

The effective charge of the projectile ion is assumed to be given by the Brown and Moak[6] relation

$$Z_B/Z_1 = 1 - 1.034 \exp \left[-V/(Z_1^{0.69} \times V_b) \right]$$

where Z_1 is the atomic number of the projectile ion and V_b is the Bohr velocity 2.188×10^8 cm/sec.

To calculate an average ionization potential for a target ion of charge q, a scheme proposed by Mehlhorn[5] was adopted;

$$<I_q> = (Z/Z_n)^2 <I_n> ,$$

where Z_n is the atomic number and $\langle I_n \rangle$ is the average ionization potential of a neutral atom with the same electronic configuration as the target ion of charge q.

Once the stopping cross section is obtained, the stopping power due to bound atomic electrons is given by

$$\left[\frac{dE}{dx}\right]_b = \frac{\rho(x)}{m_I} S_b(E)$$

where $\rho(x)$ is the mass density of target ions in the plasma at position x, and m_I is the mass of the target ion.

Stopping power due to free plasma electrons and plasma ions is calculated from the same models as used in the previous treatment of an Al target.[2] Enhanced stopping power due to collective beam effects is included, although in the case treated here, this effect is small.

III. Results

Some results of the proton beam-Fe slab target interaction simulation will now be given. Figure 1 shows the density, temperature, and average charge variations at the front and rear surfaces of the plasma as the interaction evolves. At the front surface, temperature and $\bar{Z}$ rise very quickly and attain approximate steady state values within the first few nanoseconds. The density drops rapidly at first, then drops more slowly at later times, but it is always decreasing as the plasma expands. There is some slight cooling and a noticeable drop in $\bar{Z}$ after the beam is shut off at 10 nsec. The temperature and $\bar{Z}$ rise at the rear surface is much more gradual and does not begin to level off until near the end of the beam pulse. The density decreases here also as the plasma expands. The peaks in the rear surface plots at early times are due to the arrival of a shock wave.

Density and temperature profiles at different times in the plasma evolution are shown in Fig. 2. In these plots, the beam is incident from the right. The expansion of the plasma with time is easily discerned. At early times, there are significant gradients near the rear surface. As time goes on, these variations disappear and the plasma becomes more

4

uniform, especially at about 13 nsec, three nsec after the beam has been turned off. After three nsec, the temperature throughout most of the plasma remains fairly steady. At 1.7 nsec, the beam is stopped in the plasma interior and does not reach the backside to heat it up. This is also true at later times; the temperature increase at the rear surface arises from heating due to radiation transport from the interior of the plasma.

Calculated front and rear spectra at these times are displayed in Fig. 3. The lack of level structure in the lower ionization stages is demonstrated by the paucity of lines in Fig. 3a and in the rear spectra in Figs. 3b and 3c. Lines appear in the spectra when the plasma gets hot enough so that ions with level structure have a significant abundance. The peaks in the rear spectra, except at the lowest photon energies, arise from radiation from the plasma interior "shining through" opacity "windows". The dominant contribution to the front surface spectra generally comes from the outermost zone, although "shine-through" contributions from the interior can produce some peaks in the curve. As can be noted from Figs. 1 and 2, the plasma is nearly uniform at 13.15 nsec; hence the front and rear spectra are very similar. The front spectra becomes more intense at the higher frequencies up to 10 nsec, but, as might be expected, the 13.15 nsec front spectra is less intense than at 10 nsec due to plasma cooling after beam shutoff.

Figure 4 gives the energy history and partitioning of the beam-target interaction; "dep" is the energy deposited by the beam, and "sum" is the total energy remaining in the plasma in various forms. After the beam shutoff at 10 nsec, the total, internal, and potential energies decrease as the plasma cools; only the kinetic energy continues to rise as the plasma expands. At early times, the energy lost by radiation is insignificant, but by 13 nsec, this represents about a third of the deposited energy. Thus, radiation represents a significant energy loss. If the Fe atomic model had included level structure and line radiation in the lower ionization stages, the radiation loss would be greater, particularly at early times. However, as stated earlier, this lack of line structure is presumed to have an effect of less than a factor of two on the radiation loss.

IV. Summary

The interaction of a one-MeV proton beam with an intensity of 16 terawatts/cm^2 with a planar 8.0-μm-thick iron slab has been simulated using a fully self-consistent, one-dimensional hydrodynamic-ionization-radiation transport code. An extensive atomic-level-structure model of Fe was employed, and atomic populations as functions of temperature and density were calculated from a collisional-radiative-equilibrium assumption. Radiation transport was treated with a hybrid scheme that combines a multi-frequency formalism for the continuum with a probability-of-escape method for the lines.

Profiles of the plasma density and temperature at various times in the plasma evolution, and corresponding front and rear emission spectra at these times, have been presented. Front and rear surface density, temperature, and average ionic charge has been discussed, and the energy partitioning among the various degrees of freedom has been shown.

Due to limitations of computer storage and other factors, detailed atomic structure was only included for Fe XVI and higher stages. Since the maximum average charge obtained was about 18, radiation losses are underestimated throughout the simulation; however, it is estimated that the error is less than a factor of two.

At these beam intensity levels, no K-shell emission was predicted, in contrast to the earlier study of the interaction of the same proton beam with an aluminum target.[2] Many L-shell lines are present during the latter part of the simulation.

There has been much interest recently in lasing schemes involving $2p^53p$-$2p^53s$ transitions in neonlike systems. One such transition is the $2p^53p(\frac{1}{2},\frac{1}{2})_0$-$2p^53s(\frac{1}{2},\frac{1}{2})_1$ transition at 254.9A in Fe XVII. One of the reasons for undertaking this study is to see if this transition can be excited by proton beams. The atomic model did not have detailed jj levels for Fe XVII; the 3p levels were combined into two groups according to the spin of the $2p^5(^2P)$ inner shell. Nevertheless, it should be possible to make some estimates of the feasibility of inducing this transition. After about 5.5 nsec, these 3p levels had fractional population densities of ~5-6x10^{-3} to ~10^{-2}. During this time, the ion density was of the order 10^{20},

and the electron density of the order 10^{21}. The temperatures in the plasma during these times averaged about 180 eV, with some hotter zones rising above 200 eV. Under these conditions, it should be possible to see some lasing in this line.

This treatment is one-dimensional; hence, field effects and lateral energy flow have been omitted. These factors could alter profile shapes and magnitudes, and stopping power in the plasma, and thus affect the results presented here.

V. ACKNOWLEDGMENTS

VI. REFERENCES

1. G. Maynard and C. Deutsch, Phys. Rev. A26, 665 (1982).

2. J. E. Rogerson, R. W. Clark, and J. Davis, Phys. Rev. A31, 3323 (1985); J. E. Rogerson, R. W. Clark, and J. Davis, NRL Memo Report 5482 (1984). ADA 148904

3. H. H. Anderson and J. F. Ziegler, "Hydrogen-Stopping Powers and Ranges in All Elements," Pergamon Press (1977).

4. E. J. McGuire, J. M. Peek, and L. C. Pitchford, Phys. Rev. A26, 1318 (1982).

5. T. A. Mehlhorn, J. Appl. Phys. 52, 6522 (1981).

6. M. D. Brown and C. D. Moak, Phys. Rev. B6, 90 (1972).
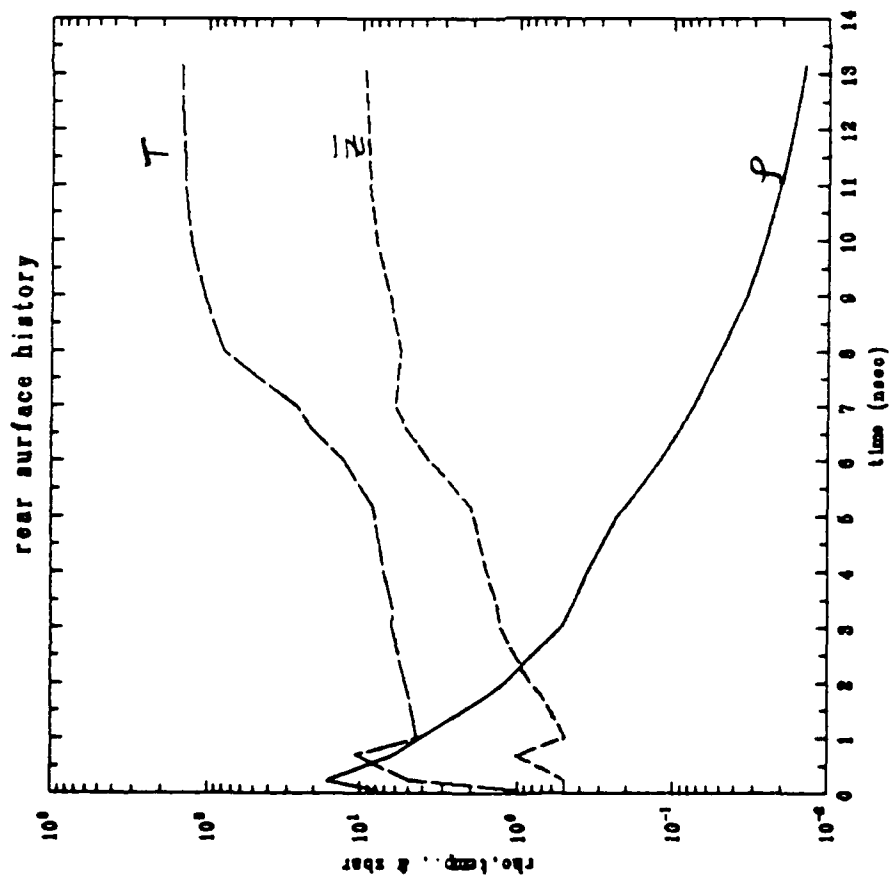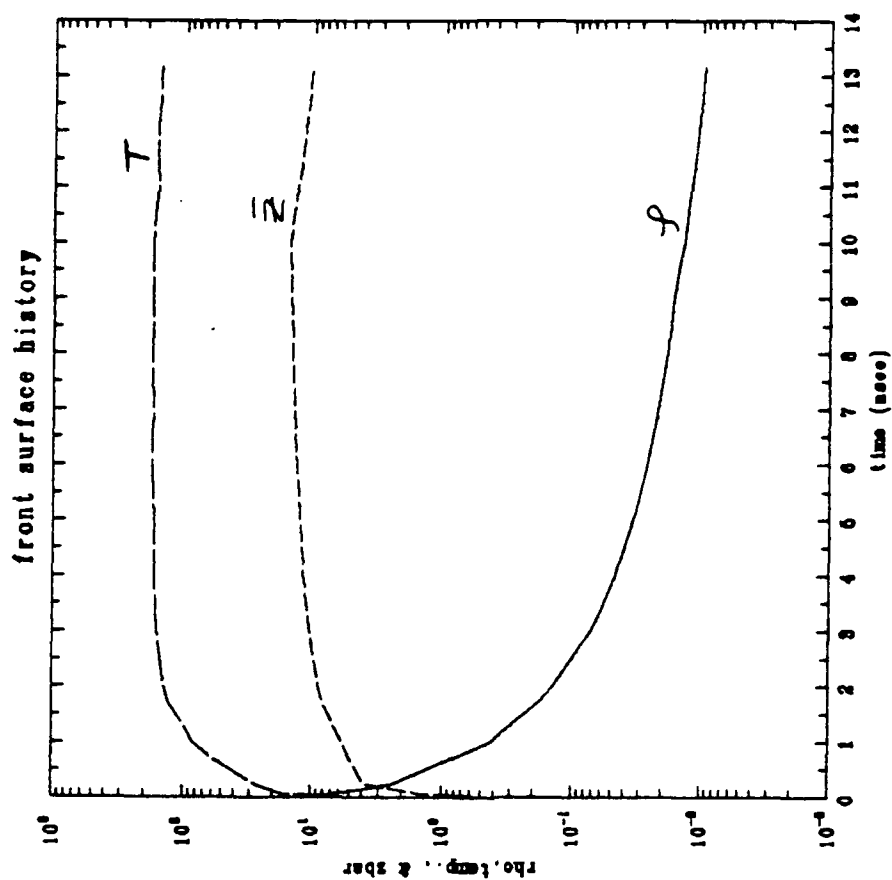
Fig. 1 Temperature, density, and average charge variation at the front and rear surfaces with time.
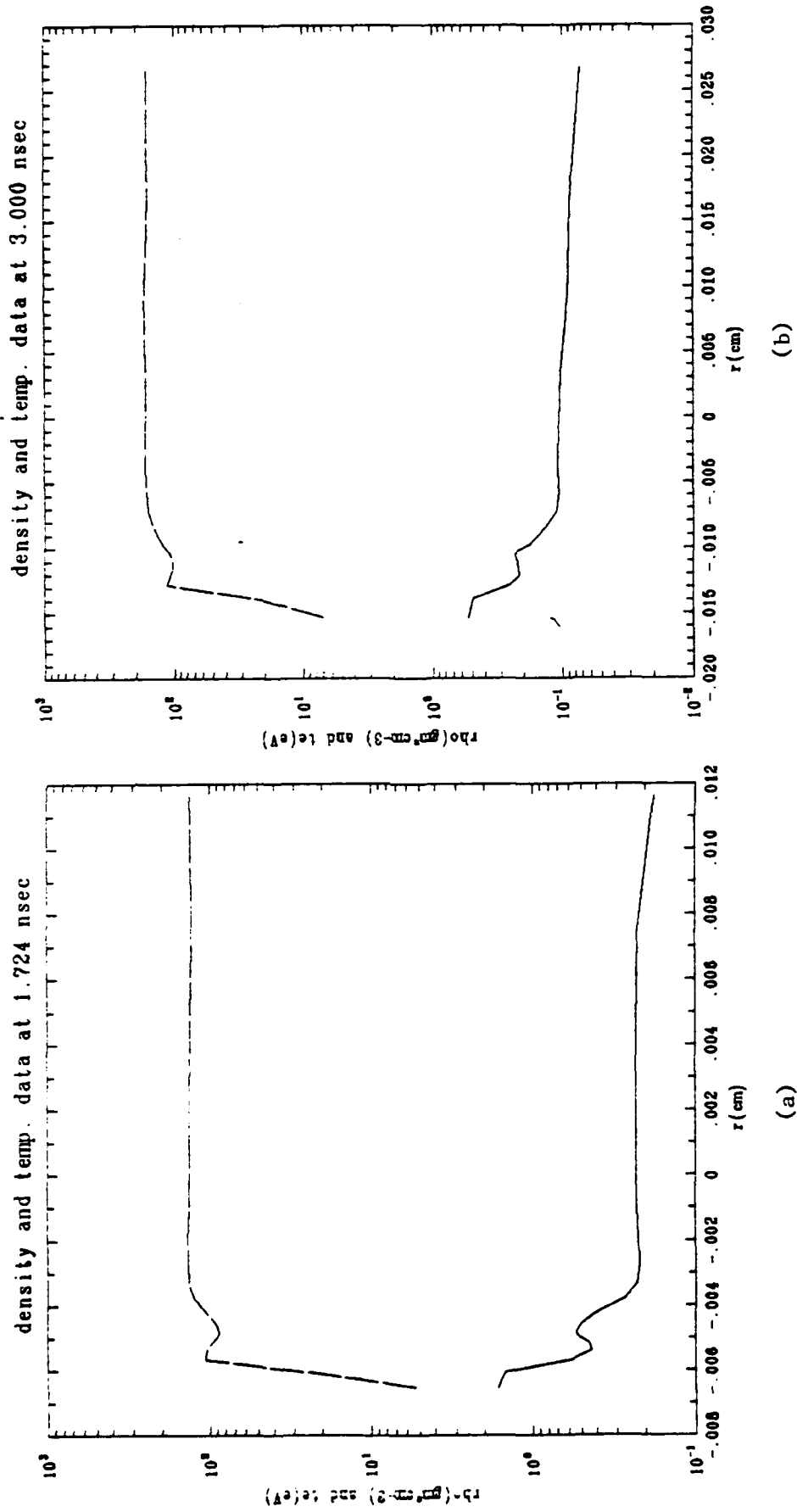
Fig. 2 Density and temperature profiles at different times in the plasma evolution.
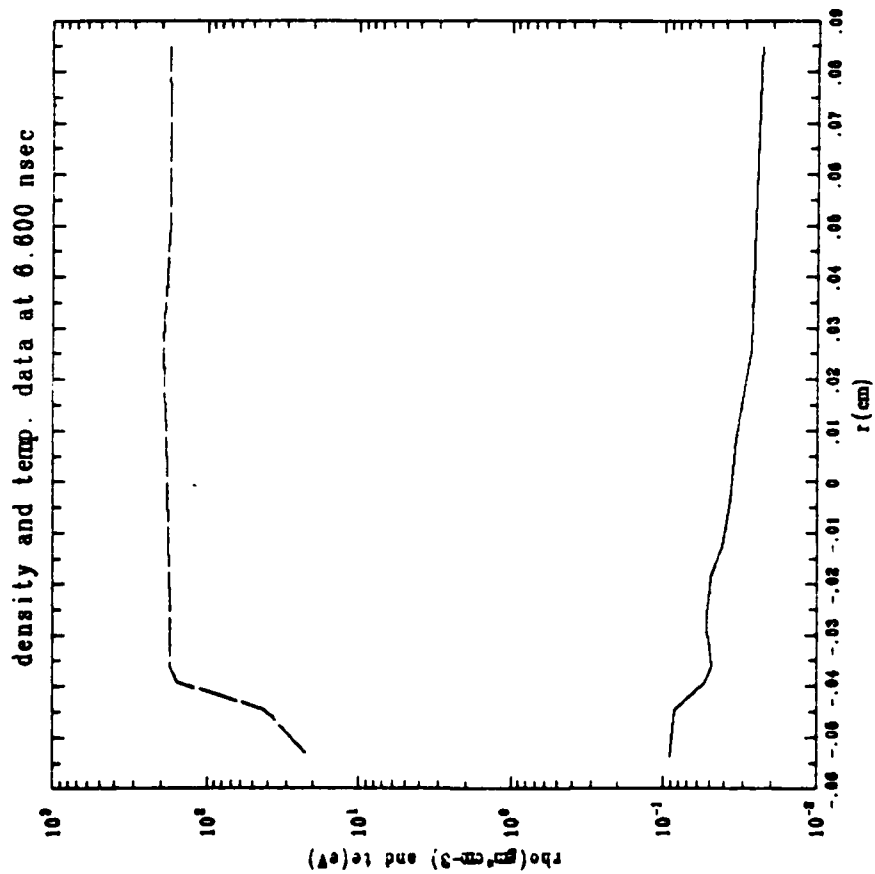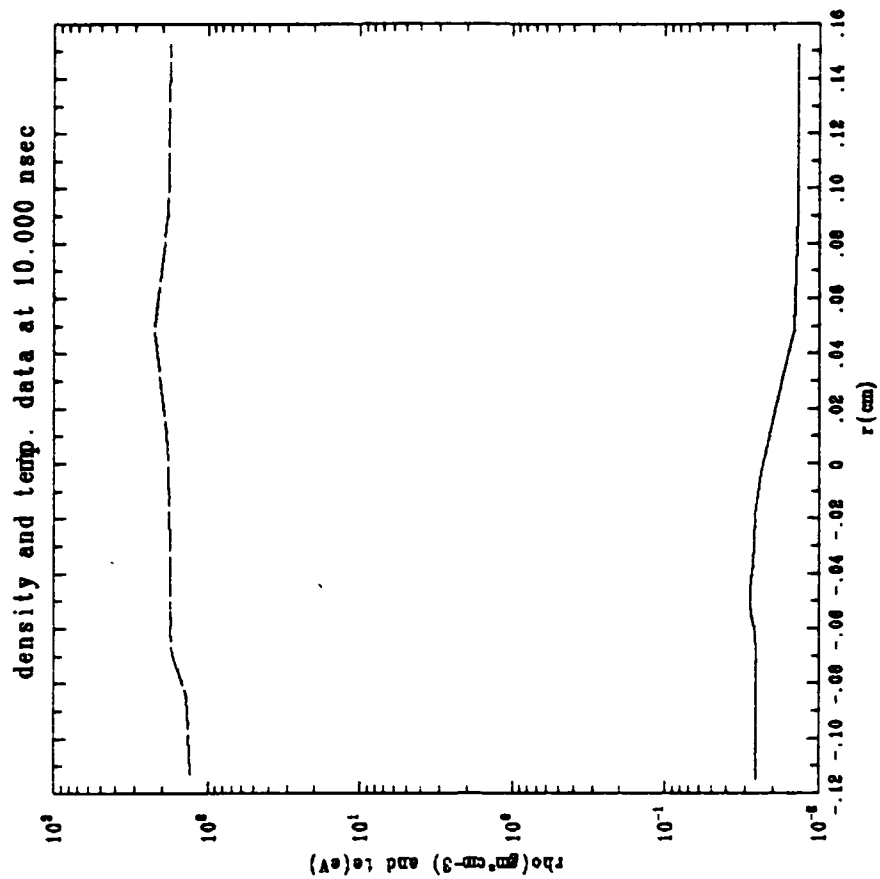
density and temp. data at 10.000 nsec

rho(gr.cm-3) and te(eV)

r(cm)

(d)

density and temp. data at 6.600 nsec

rho(gr.cm-3) and te(eV)

r(cm)

(c)

Fig. 2 (Continued) Density and temperature profiles at different times in the plasma evolution.

density and temp. data at 13.146 nsec

(e)

Fig. 2 (Continued) Density and temperature profiles at different times in the plasma evolution.

11

front and rear spectra at 3.000 nsec

(b)

spectral intensity(w/kev/cm2)

photon energy(kev)

front and rear spectra at 1.724 nsec

(a)

spectral intensity(w/kev/cm2)

photon energy(kev)

Fig. 3 Front and rear emission spectra at various times in the plasma evolution.

12

Fig. 3 (Continued) Front and rear emission spectra at various times in the plasma evolution.

13

front and rear spectra at 13.146 nsec
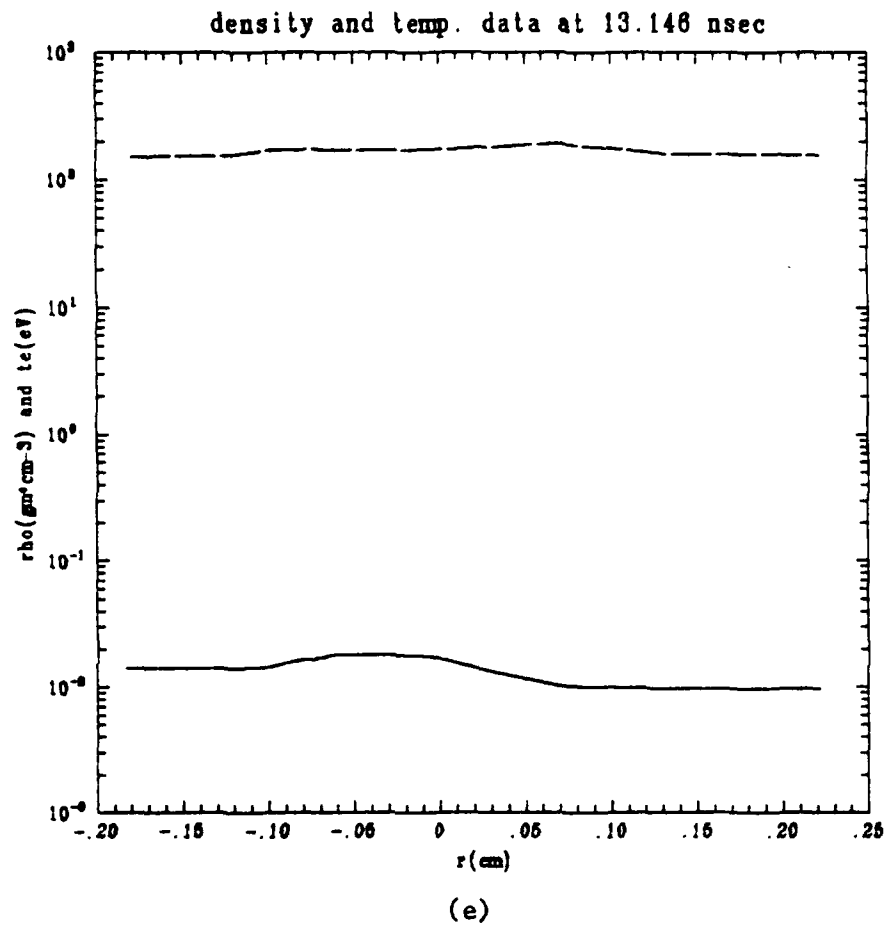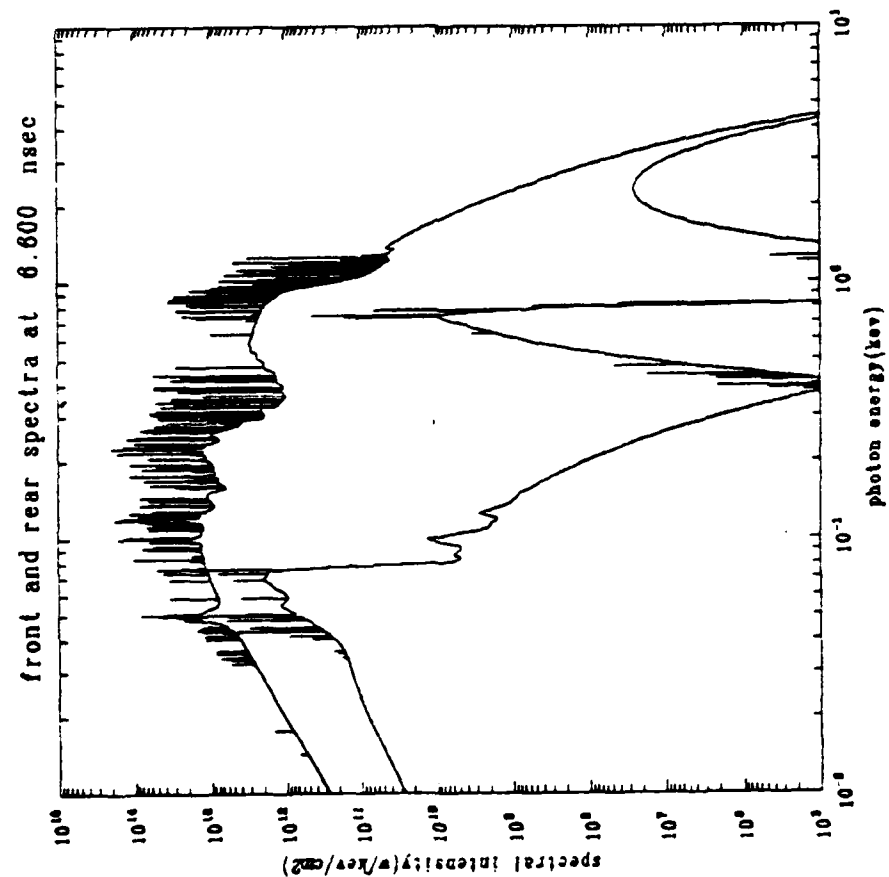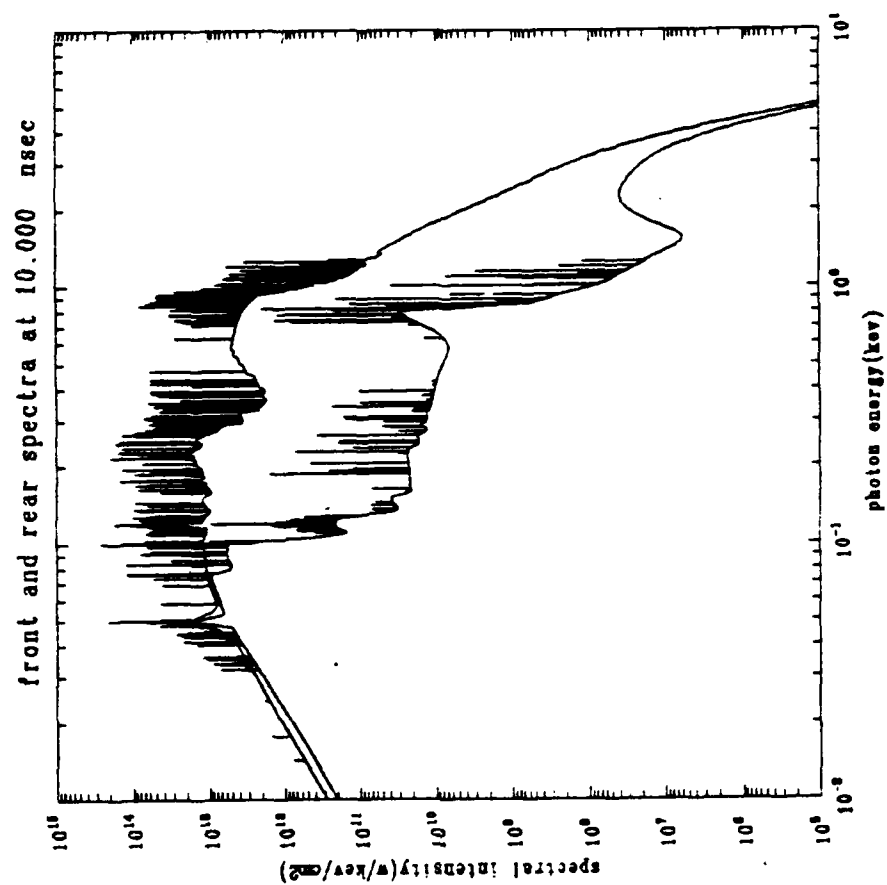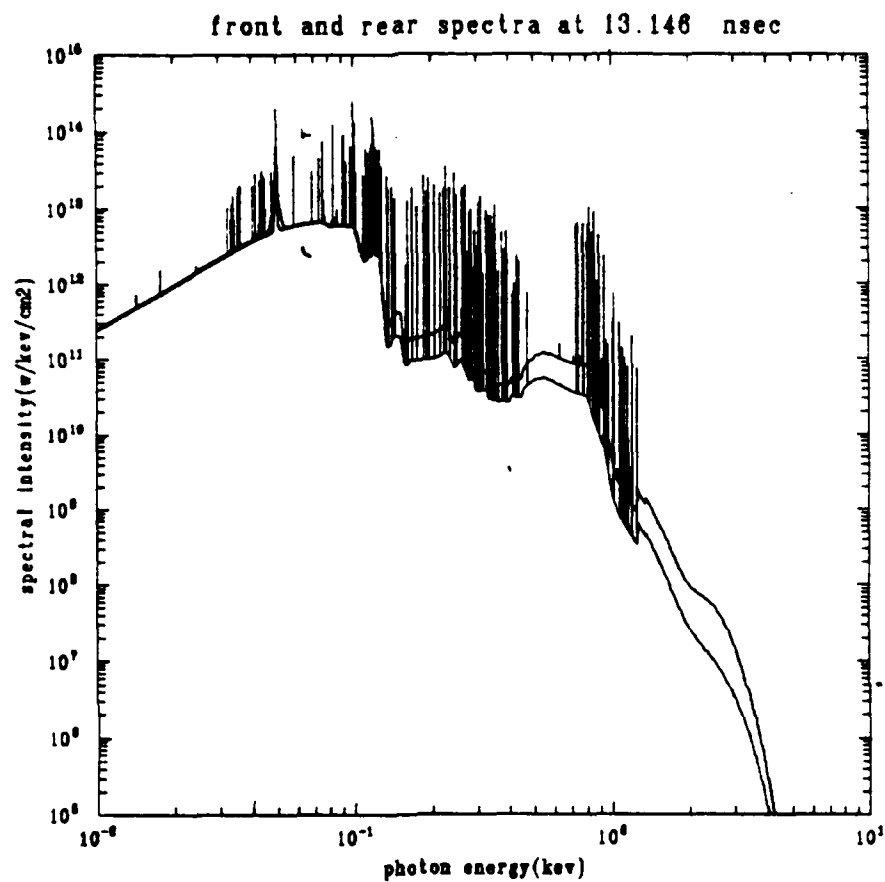
(e)

Fig. 3 (Continued) Front and rear emission spectra at various times in the plasma evolution.
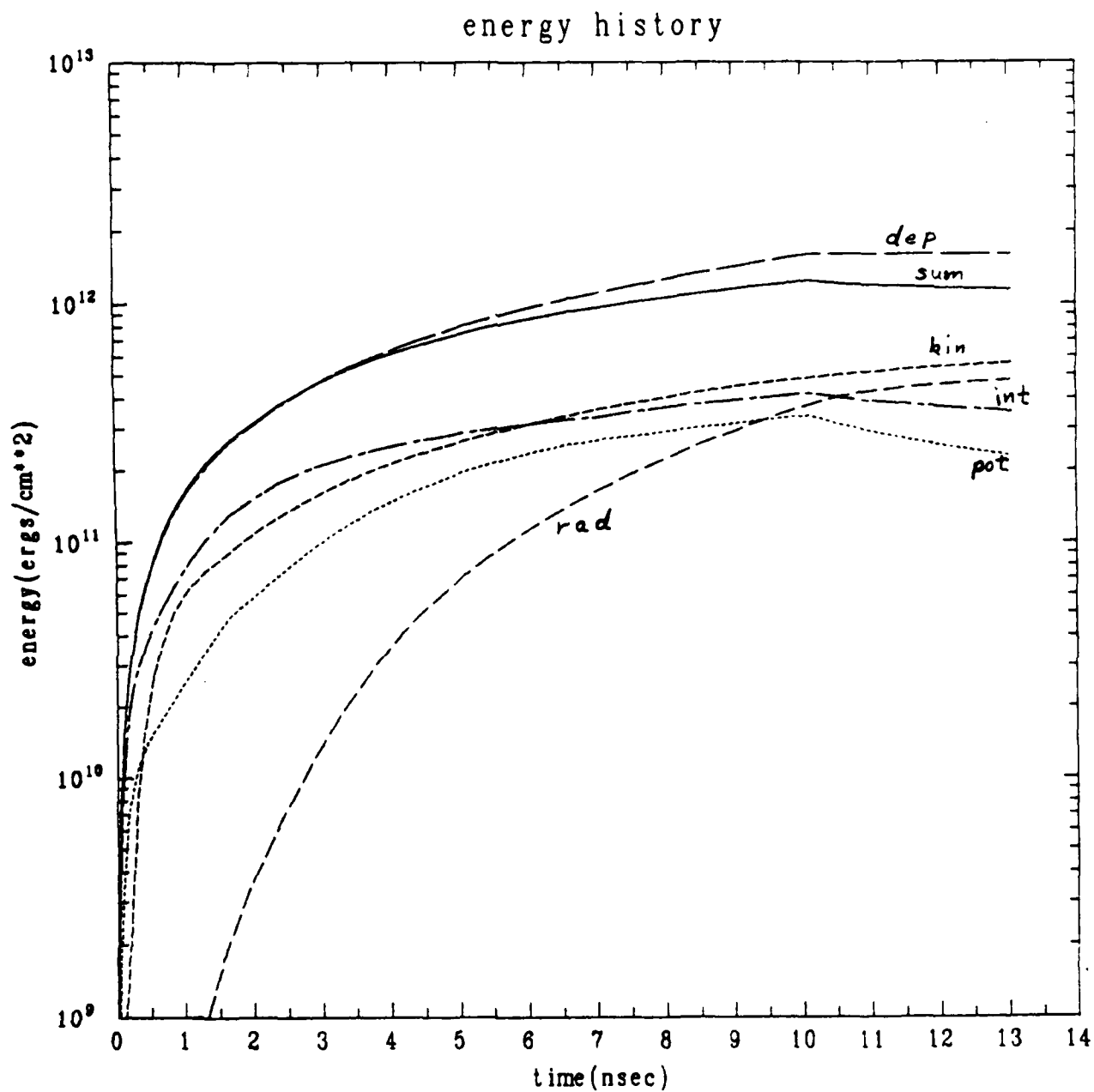
energy history

Fig. 4 Energy history of the beam-plasma evolution.

DISTRIBUTION LIST

Assistant to the Secretary of Defense   1 Copy
Atomic Energy
Washington, D.C. 20301
    ATTN: Executive Assistant

Director   1 Copy
Defense Intelligence Agency
Washington, D.C. 20301
    ATTN: DT-1B R. Rubenstein

Director
Defense Nuclear Agency
Washington, D.C. 20305
    ATTN: DDST   1 copy
    ATTN: TITL   4 copies
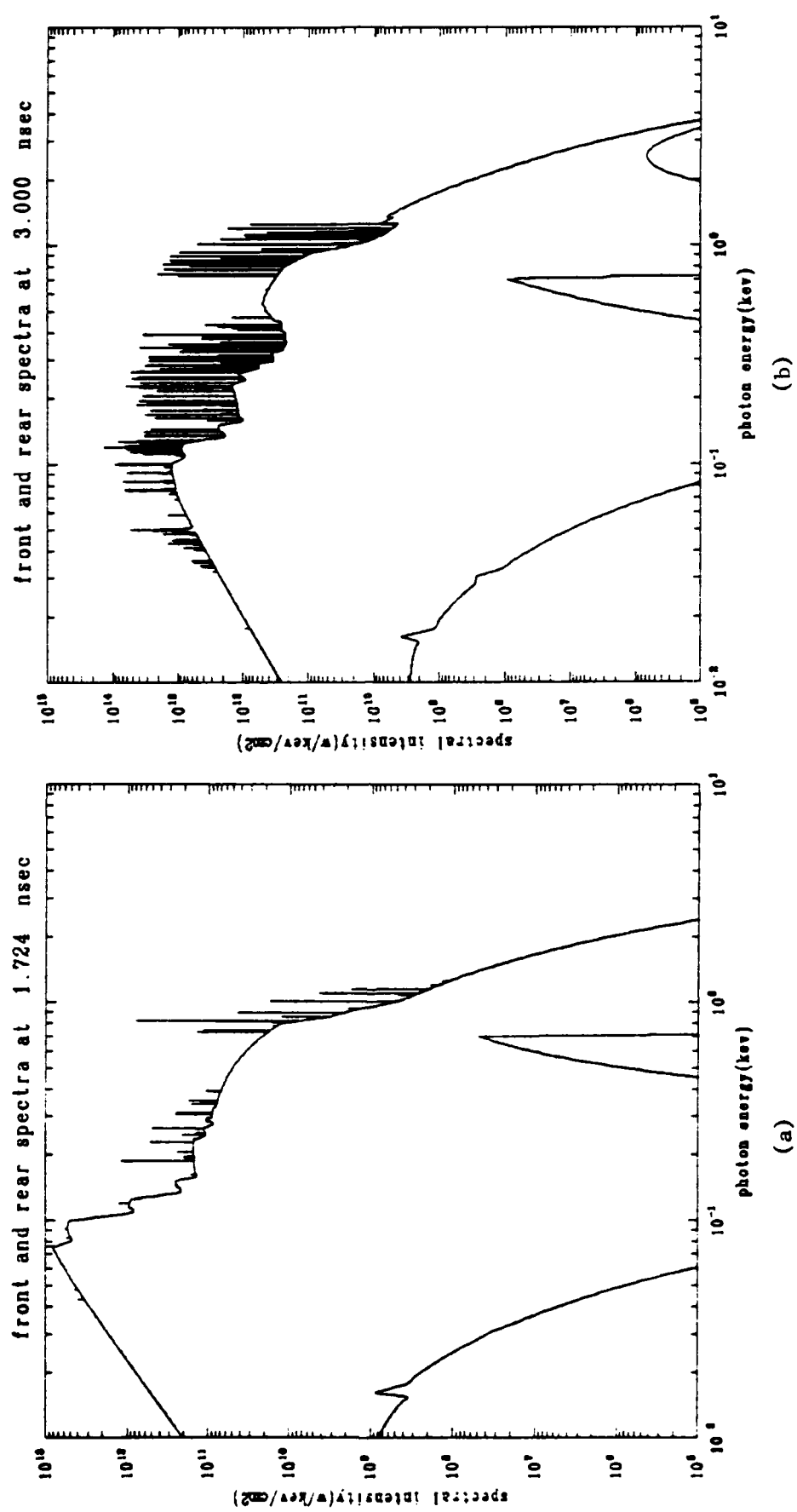   ATTN: RAEV   1 copy
    ATTN: STVI   1 copy

Commander   1 Copy
Field Command
Defense Nuclear Agency
Kirtland AFB, New Mexico 87115   .
    ATTN: FCPR

Chief   1 Copy
Field Command
Livermore Division
Department of Defense
P.O. Box 808
Livermore, CA 94550
    ATTN: FCPRL

Director   1 Copy
Joint Strat TGT Planning Staff
Offutt AFB
Omaha, Nebraska 68113
    ATTN: JLKS

Undersecretary of Defense   1 Copy
for RSCH and ENGRG
Department of Defense
Washington, D.C. 20301
    ATTN: Strategic and Space Systems (OS)

Deputy Chief of Staff for RSCH DEV and ACQ   1 Copy
Department of the Army
Washington, D.C. 20301
    ATTN: DAMA-CSS-N

17

```
Commander                                             1 copy each
Harry Diamond Laboratories
Department of the Army
2800 Powder Mill Road
Adelphi, MD  20783
     ATTN:  DELHD-N-NP
     ATTN:  DELHD-R J. Rosado
     ATTN:  DELHD-TA-L (Tech. Lib.)


U.S. Army Missile Command
Redstone Scientific Information Center               3 Copies
Attn:  DRSMI-RPRD (Documents)
Redstone Arsenal, Alabama  35809


Commander                                             1 copy
U.S. Army Missile Command
Redstone Arsenal, Alabama  35898
     ATTN:  DRCPM-PE-EA


Commander
U.S. Army Nuclear and Chemical Agency
7500 Backlick Road                                    1 copy
Building 2073
Springfield, VA  22150
     ATTN:  Library


Commander                                             1 Copy
Naval Intelligence Support Center
4301 Suitland Road, Bldg. 5
Washington, D.C. 20390
     ATTN:  NISC-45


Commander                                             1 Copy
Naval Weapons Center
China Lake, California  93555
     ATTN: Code 233 (Tech. Lib.)


Officer in Charge                                     1 Copy each
White Oak Laboratory
Naval Surface Weapons Center
Silver Spring, Md.  20910
     ATTN: Code R40
     ATTN: Code F31


Air Force Weapons Laboratory                          1 Copy each
Kirtland AFB, New Mexico  87117
     ATTN:  SUL
     ATTN:  CA
     ATTN:  APL
     ATTN:  Lt. Col Generosa
```

18

```
Deputy Chief of Staff                              1 Copy
Research, Development and Accounting
Department of the Air Force
Washington, D. C. 20330
     ATTN:  AFRDQSM


Commander                                          1 Copy
U.S. Army Test and Evaluation Command
Aberdeen Proving Ground, MD  21005
     ATTN: DRSTE-EL


AVCO Research and Systems Group                    1 Copy
201 Lowell Street
Wilminton, MA  01387
     ATTN:  Library A830


BDM Corporation                                    1 Copy
7915 Jones Branch Drive
McLean, Virginia  22101
     ATTN:  Corporate Library


Berkeley Research Associates                       1 Copy
P.O. Box 983
Berkeley, CA  94701
     ATTN:  Dr. Joseph Workman


Berkeley Research Associates                       1 Copy each
P.O. Box 852
5532 Hempstead Way
Springfield, VA  22151
     ATTN:  Dr. Joseph Orens


Boeing Company                                     1 Copy
P. O. Box 3707
Seattle, WA  98134
     ATTN:  Aerospace Library


The Dikewood Corporation                           1 Copy
1613 University Bldv., N.E.
Albuquerque, New Mexico  87110
     ATTN:  L. Wayne Davis


General Electric Company                           1 Copy
Space Division
Valley Forge Space Center
P. O. Box 8555
Philadelphia, PA  19101
     ATTN:  J. Peden
```

General Electric Company - Tempo   1 Copy
Center for Advanced Studies
816 State Street
P.O. Drawer QQ
Santa Barbara, CA 93102
    ATTN: DASIAC

Institute for Defense Analyses   1 Copy
1801 N. Beauregard St.
Alexandria, VA 22311
    ATTN: Classified Library

IRT Corporation   1 Copy
P.O. Box 81087
San Diego, CA 92138
    ATTN: R. Mertz

JAYCOR   1 Copy
11011 Forreyane Rd.
P.O. Box 85154
San Diego, CA 92138
    ATTN: E. Wenaas
           F. Felbar

JAYCOR   1 Copy
205 S. Whiting Street, Suite 500
Alexandria, VA 22304
    ATTN: R. Sullivan

KAMAN Sciences Corp.   1 copy each
P. O. Box 7463
Colorado Springs, CO 80933
    ATTN: Library

Lawrence Livermore National Laboratory   1 copy each
University of California
P.O. Box 808
Livermore, California 94550
    Attn: DOC CDN for L-153
    Attn: DOC CDN for L-47 L. Wouters
    Attn: DOC CDN for Tech. Infor. Dept. Lib.

Lockheed Missiles and Space Co., Inc.   1 copy each
P. O. Box 504
Sunnyvale, CA 94086
    Attn: S. Taimlty
    Attn: J.D. Weisner

Lockheed Missiles and Space Co., Inc.   1 Copy
3251 Hanover Street
Palo Alto, CA 94304
    Attn: J. Perez

20

Maxwell Laboratory, Inc.   1 Copy each
9244 Balboa Avenue
San Diego, CA 92123
     ATTN: A. Kolb
     ATTN: M. Montgomery
     ATTN: J. Shannon

McDonnell Douglas Corp.   1 Copy
5301 Bolsa Avenue
Huntington Beach, CA 92647
     ATTN: S. Schneider

Mission Research Corp.   1 Copy each
P. O. Drawer 719
Santa Barbara, CA 93102
     ATTN: C. Longmire
     ATTN: W. Hart

Mission Research Corp.-San Diego   1 Copy
5434 Ruffin Rd.
San Diego, California 92123
     ATTN: Victor J. Van Lint

Northrop Corporation   1 Copy
Northrop Research and Technology Center
1 Research Park
Palos Verdes Peninsula, CA 90274
     ATTN: Library

Physics International Company   1 Copy each
2700 Merced Street
San Leandro, CA 94577
     ATTN: M. Krishnan
     ATTN: C. Gilman
     ATTN: S. Wong

R and D Associates   1 Copy each
P.O. Box 9695
Marina Del Rey, CA 90291
     ATTN: W. Graham, Jr.
     ATTN: P. Haas

Sandia National Laboratories   1 copy each
P.O. Box 5800
Albuquerque, New Mexico 87115
     ATTN: Doc Con For 3141
     ATTN: D. McDaniel
     ATTN: P. VanDevender
     ATTN: K. Matzen, Code 4247

Science Applications, Inc.   1 copy
P. O. Box 2351
La Jolla, CA 92038
     ATTN: R. Beyster

21

Spectra Technol, Inc.,   1 copy
Attn: Alan Hoffman
2755 Northup Way
Bellevue, Washington 98004

Spire Corporation   1 copy
P. O. Box D
Bedford, MA 01730
    ATTN: R. Little

SRI International   1 copy
333 Ravenswood Avenue
Menlo Park, CA 94025
    ATTN: S. Dairiki

S-CUBED   1 copy
P. O. Box 1620
La Jolla, CA 92038
    ATTN: A. Wilson

Director
Strategic Defense Initiative Organization   1 copy each
1717 H Street
Pentagon 20301-7100
    ATTN: DE   Lt. Col Richard Gullickson/DEO
           IST Dr. Dwight Duston
    ATTN: IST Dr. J. Ionson

Texas Tech University   1 copy
P.O. Box 5404
North College Station
Lubbock, TX 79417
    ATTN: T. Simpson

TRW Defense and Space Systems Group   1 Copy
One Space Park
Redondo Beach, CA 90278
    ATTN: Technical Information Center

University of Buffalo
Attn: Professor W. J. Sarjeant   1 Copy
Dept. of Electrical Engineering
High Voltage and Power
312 Bonner Hall
Buffalo, New York 14260

Naval Research Laboratory
Plasma Radiation Branch
Washington, D.C. 20375
      Code 4720   -   50 Copies
      Code 4700   -   26 Copies
      Code 2628   -   22 Copies

END

11-86

DTIC